

Modeling time variation of blood temperature in bioheat equation and its application to temperature analysis due to RF exposure

Akimasa Hirata and Osamu Fujiwara

Corresponding Author: Akimasa Hirata (ahirata@nitech.ac.jp)

Department of Computer Science and Technology, Nagoya Institute of Technology, Showa-ku, Nagoya 466-8555, Japan

Abstract

The present study discusses a scheme to take into account core temperature variation in a well-known bioheat equation. First, the limitation in conventional modeling of the bioheat equation was investigated for a problem in which the whole-body phantom should be taken into account. Then, schemes for varying body-core temperature in the bioheat equation were discussed for radio-frequency exposures. The computational uncertainty in the core temperature elevation is found to be reasonable when a proper scheme for computing the net rate of heat acquisition by blood from body tissue was introduced.

1. Introduction

There has been increasing public concern about adverse health effects caused by electromagnetic exposures. Much attention has been paid to radio-frequencies (RFs), among others, since they are being widely used in wireless communication systems. RFs are also applied in some therapy and diagnostic procedures, e.g., magnetic resonance diagnosis and hyperthermia. The most dominant effect of RF on humans is known to be thermal, or the temperature elevation due to RF energy absorption (ICNIRP, 1998).

When analyzing the temperature variation in humans and animals due to RF energy, a well-known bioheat equation (Pennes 1948) is often applied, as in cases of hyperthermia (Saito *et al* 2004), magnetic resonance devices (Nguyen *et al* 2004), and RF far-field exposures (Bernardi *et al* 2003, Hirata *et al* 2007, 2008). The bioheat equation would be a reasonable and powerful tool to analyze the temperature in the shallow region of the body (Nelson 1998, Wissler 1998). However, the first law of thermodynamics is not satisfied since the heat removed from tissue with blood perfusion vanishes in a conventional formulation of the bioheat equation. This violation would not be essential when the RF energy deposition in the body is smaller than the total amount of the basal metabolism. For whole-body exposure and intense localized exposure, the body-core temperature elevates with time. (e.g., see Guy *et al* (1975) in rabbits exposed to intense localized exposures). To analyze the temperature in the body for whole-body RF exposure, Bernardi *et al* treated the blood temperature in the bioheat equation as a variable over time in order to take into account the energy deposited in the blood (Bernardi *et al* 2003). We have presented a similar formula for blood temperature (Hirata *et al* 2006). Note that the blood temperature is assumed to be constant over the whole body since the blood circulates throughout the human body in one minute or less (Follow and Neil 1971). However, no detailed discussion of their effectiveness has been given in these studies. Recently, the computational error due to the discretization of the term associated with heat conduction in the bioheat equation has been investigated by Bernardi *et al* (2003) and Samaras *et al* (2006). Its influence on core temperature elevation has not been well understood.

In the present study, we first revealed a fundamental limitation of the conventional bioheat equation due to an assumption that the blood temperature is spatially constant. Based on that discussion, we investigated different schemes to vary blood or core temperature in the bioheat equation. The effectiveness of the schemes was discussed by comparison with measurements in earlier works which investigate the temperature elevation in rabbits exposed to RF far-fields (Hirata *et al* 2008).

2. Model and Methods

2.1. Computational methods

The bioheat equation is often used for calculating temperature elevation in numeric phantoms (Pennes 1948). A generalized bioheat equation is given by the following:

$$C(\mathbf{r})\rho(\mathbf{r})\frac{\partial T(\mathbf{r},t)}{\partial t} = \nabla \cdot (K(\mathbf{r})\nabla T(\mathbf{r},t)) + \rho(\mathbf{r})SAR(\mathbf{r}) + A(\mathbf{r},t) - B(\mathbf{r},t)(T(\mathbf{r},t) - T_B(\mathbf{r},t)) \quad (1)$$

where $T(\mathbf{r},t)$ and $T_B(\mathbf{r},t)$ denote the temperatures of tissue and blood, respectively, where \mathbf{r} and t are the position vector and the time. C represents the specific heat of tissue, K is the thermal conductivity of tissue, A is the basal metabolism per unit volume, and B is the term associated with blood perfusion.

The boundary condition between air and tissue for (1) is given by the following equation:

$$-K(\mathbf{r})\frac{\partial T(\mathbf{r},t)}{\partial n} = H \cdot (T_s(\mathbf{r},t) - T_e(t)) \quad (2)$$

where H , T_s , and T_e denote, respectively, the heat transfer coefficient including the effect of radiative and convective heat loss, body surface temperature, and air temperature. Hirata *et al* (2008) discussed the heat transfer coefficient between the skin and air. They subdivided the skin into two parts: ear lobe and the other parts. In Marai *et al* (2002), the average temperature of skin and ear lobe were reported to be 38.6 °C and 33.8 °C, respectively, at the air temperature of 25 °C. At that time, rectal temperature was 39.5 °C. For these values, we determined 0.65 W/m²·°C and 2.5 W/m²·°C as the respective values of the heat transfer coefficient between the skin and the air and between the ear lobe and the air. We used these values in the present study.

In conventional modeling, the blood temperature in (1) was assumed to be constant: $T_B(\mathbf{r},t) = T_{B0}$ where T_{B0} is the blood temperature given in the state without heat load or RF absorption. In addition, the basal metabolism rate and the term associated with blood perfusion are often assumed to be constant, although some recent studies have taken into account this kind of response (e.g., Bernardi *et al* 2003, Wainwright 2003, Hirata *et al* 2007). The present study does not discuss the effect of physiological modeling on core temperature, since it marginally influences core temperature in rabbits, as can be seen from an empirical equation of heat balance (Adair 2003, Ebert *et al* 2005, Hirata *et al* 2008).

The discrete vasculature thermal model, which allows for the effect of individual vessels, was proposed by Kotte *et al* (1996), in which the spatial distribution of blood temperature is considered quite naturally. However, a complex process is required to develop vascular distributions. This is one of the main reasons why the spatial distribution of blood temperature is not considered here. With regard to the core temperature and temperature in the shallow region, the assumption that the blood temperature is spatially constant would be reasonable. The effectiveness of this approach has been validated by comparison with rabbit (Hirata *et al* 2008a) and human measurements (Hirata *et al* 2008b).

In order to take into account the core temperature elevation in the bioheat equation, it is

reasonable to consider the blood temperature as a variable of time $T_B(\mathbf{r},t) = T_B(t)$, thus, the blood temperature is assumed to be constant over the whole body since the blood circulates throughout the human body in one minute or less (Follow and Neil 1971). The blood circulation time in rabbits is much smaller than that of humans due to its smaller body and larger blood perfusion rate. The blood temperature variation is given by the following equation (Bernardi *et al* 2003, Hirata *et al* 2006):

$$T_B(t) = T_{B0} + \int_t \frac{Q_{BT}(t)}{C_B \rho_B V_B} dt \quad (3)$$

where Q_{BT} is the rate of heat acquisition of the blood from the body tissues. C_B (=4000 J/kg · K), ρ_B (=1050 kg/m³), and V_B denote the specific heat, mass density, and total volume of blood, respectively. This is because $Q_{BT}(0)$ is not zero even at time $t=0$, which is attributed to some computational simplification or assumption. Thus, the following equation (4) was introduced to compensate for an unphysical time evolution of the blood temperature (Hirata *et al* 2007). The difference between (3) and (4) is that the latter evaluates the *net* rate of heat acquisition of blood from body tissues.

$$T_B(t) = T_{B0} + \int_t \frac{Q_{BT}(t) - Q_{BT}(0)}{C_B \rho_B V_B} dt \quad (4)$$

The rationale for introducing equation (4) is due to the uncertainty of initial thermal parameters, which will be discussed in Sec. 3.

The following two auxiliary equations were used to compute the rate of heat acquisition of blood from body tissues:

$$Q_{BT}(t) = \int_V B(t)(T_B(t) - T(\mathbf{r},t))dV \quad (5)$$

$$Q_{BT}(t) = \int_V (\rho(\mathbf{r})SAR(\mathbf{r}) + A(\mathbf{r},t) - C(\mathbf{r})\rho(\mathbf{r})\frac{\partial T(\mathbf{r},t)}{\partial t})dV - \oint_S H \cdot (T_s(\mathbf{r},t) - T_e(t))dS \quad (6)$$

where (5) is the formula given in (Bernardi 2003), and (6) is another expression of (5), which is derived so that the heat transfer between human body and external air satisfies the first law of thermodynamics based on equations (1) and (2). These two equations should be theoretically identical, while their difference will be discussed in the next section from the aspect of computational physics.

2.2 Numeric phantom

A numeric rabbit phantom based on CT images was used (Wake *et al* 2007). The resolution of the phantom is 1 mm and comprises of 12 tissues. In order to match the average weight of rabbits employed in the measurement (Hirata *et al* 2008) and that of the phantom, we linearly reduce the cell size of the rabbit phantom from 1 mm to 0.93 mm. The weight of the reduced rabbit is 2.0 kg. The electrical and thermal constants of the tissues were taken from our previous

study.

2.3 Computational and experimental scenario

We used a horn antenna as a source in Hirata *et al* (2008). The frequency was 2.45 GHz. The radiated fields cannot be considered as a plane wave. In order to estimate the effective power incident to a rabbit, we measured the electric field in the region of a rabbit using a probe with a resolution of 50 or 100 mm. From our measurement, the corresponding average power density was 230 W m^{-2} . Rabbits were irradiated from the lateral side. The detailed description of this exposure condition can be found in Hirata *et al* (2008). In our computation, the plane wave is given with the above equivalent power density. The blood temperature at the thermally steady state without RF exposure was put at 38.8°C so as to coincide with that of the measured rabbit.

3. Computational Results

We discuss below the fundamental limitation of conventional bioheat modeling when considering the whole-body phantom. First, the power per unit mass in (1) and that per unit area in (2) were integrated, and then evaluated at the thermally steady state without RF exposure. Note that the initial temperature distribution was calculated by giving the blood temperature of 38.8°C without equations (3) or (4).

Figure 1 shows these powers in the whole rabbit phantom at that steady state. Two discretization schemes were considered for the term associated with heat conduction. One is the conventional modeling and the other is a model improved by Bernardi *et al* (2003) and Samaras *et al* (2006). Due to the uncertainty of the heat transfer coefficient at the body surface (e.g., Hirata *et al* (2006)), we considered it as a variable in figure 1. The basal metabolism of the rabbit phantom is 8 W, or a basal metabolic rate of 4 W kg^{-1} for the parameters given in Hirata *et al* (2006). In figure 1, the first term on the right-hand side of (1) is dependent on the heat transfer coefficients for the conventional discretization scheme of heat conductivity. The volume integral of this term must be zero to satisfy the divergence theorem. The volume integral of this term becomes almost zero when using the scheme improved by Bernardi *et al* (2003) and Samaras *et al* (2006). Thus, the conventional discretization scheme would cause a computational error, resulting in a heat unbalance throughout the body. This figure also suggests that the term associated with blood perfusion behaves as a heat source for a typical set of parameters, although there is no net gain or loss from blood in humans and animals. This unphysical behavior is caused by the assumption that the blood perfusion rate is assumed to be spatially constant. A more thorough discussion will be made in the next section.

Next, we discuss the effect of computational formulas on core temperature variation in a rabbit exposed to RF fields. Figure 2 shows the time evolution of the blood temperature in the rabbit

phantom with different formulas. Attention is paid to i) the effect of the compensation scheme of blood temperature (4), ii) the effect of discretization schemes associated with heat conduction, and iii) the effect of the computational scheme for the rate of heat acquisition by the blood from body tissues ((5) or (6)). Heat transfer coefficients of 0.8 and $1.5 \text{ W m}^{-2} \text{ K}^{-1}$ were chosen. Note that the heat in the body becomes almost balanced at the former heat transfer coefficient, while the latter was chosen for comparison. These values are well within the range measured in Hirata *et al* (2006).

First, let us investigate the temperature elevation for an ideal computational condition. Figure 2 (a) shows the temperature elevation with the heat transfer coefficient $H=0.8 \text{ W m}^{-2} \text{ K}^{-1}$ and with the improved discretization scheme. As seen from this figure, all the curves almost coincide with each other. A slight difference of 3% was observed by the introduction of the compensation scheme for the blood temperature (4). Note that the results with equation (3) became identical to those with equation (4) when using the heat transfer coefficient $H=0.76 \text{ W m}^{-2} \text{ K}^{-1}$. These curves also coincide with measured temperature, and thus the result with the improved discretization scheme and with eq. (4) is considered as a reference value.

In order to clarify the effect of i), we considered the same scenario as in Figure 2 (b) except for the heat transfer coefficient of $H=1.5 \text{ W m}^{-2} \text{ K}^{-1}$, which is well within the uncertainty range estimated from the measured data. The results are given in figure 2(b). Compared with the core temperature in figures 2(a) and (b), the difference caused by i) was found to be 35% when using Eq. (3), while at most 4% when using Eq. (4). This comparison suggests that the computational result with Eq. (4) provides a reasonable result even when the heat in the body does not achieve balanced. From the same figure, the effect of computational scheme of the rate of heat acquisition of blood from body tissues does not influence the computational results (with Eqs (5) or (6)), as is the same as figure 2 (a). When changing the total basal metabolism by 10% or so, the same tendency was observed, although the computational results are not shown to avoid repetition.

In order to discuss the effect of (ii), we show the computational results for the same computational conditions with figures 2 (a) and (b) except for the discretization scheme of heat conduction. As seen from figure 2 (c), the computational error becomes obvious due to the discretization scheme. The differences with the reference value become obvious; 3% for the condition with Eqs. (4) and (6), 9% for Eqs. (4) and (5), 11% for Eqs. (3) and (6), and 19% for Eqs. (3) and (5). The same tendency was observed in figure 2 (d), but the differences are much larger than those in figure 2 (c) because of the different heat transfer coefficient.

Finally, we discuss the effect of the computational scheme for the rate of heat acquisition by the blood from body tissues. As mentioned above, this term influences the computational results only when the improved discretization scheme for heat conductivity is not introduced. When

compared to the curves of equations (5) and (6) in figure 2(c) and (d), the difference in the core temperature elevation due to this factor was found to be 6-9%.

IV. Discussion

From figure 1, the power transferred from the body to the air and the basal metabolism must be balanced in the thermally steady state. They do not balance, however, for typical sets of thermal parameters. There are several reasons for this discrepancy. One is due to the assumption that the blood temperature is spatially uniform. Specifically, the body-core temperature is used even in the shallow regions of the body, such as skin layers. This assumption can be more problematic for humans, since the temperature at the body surface and body core is largely different, unlike small animals, such as rabbits (Marai *et al* 2001). The second is due to the uncertainty of the basal metabolism/blood perfusion rate of tissues, which depends on the individual and body parts. Note that the blood perfusion rate and basal metabolism of tissues are proportional to each other (Gordon *et al* 1976). In addition, the number of tissues considered in the rabbit is limited to 12 in our numeric phantom. Third, there is some difference between the surface area of a numeric model and that in an actual body, which is attributed to the discretization of the body surface (Samaras *et al*, 2006). This effect can be compensated by using a revised heat transfer coefficient, just as in Neufeld *et al* (2007). The actual heat transfer coefficients would be smaller than these values by a factor of 1.4 or less (Samaras *et al* 2006). For a typical set of thermal parameters, therefore, the blood behaves as a heat source to satisfy the thermodynamic law.

It is quite difficult to choose a set of thermal parameters for different RF exposure scenarios. As seen from figure 2, the dominant factor influencing the computed core temperature elevation is whether the (4) is applied or not. The application of the improved discretization scheme for the term associated with the heat conduction was found to suppress the computational error by 6-9%. If this improved scheme was not applied, additional error would be caused by the formula computing the rate of heat acquisition by blood from body tissues. In particular, the error may be larger than 50% as in figure 2(d), when no compensation scheme is implemented.

IV. SUMMARY

In the present study, we discussed some problems in the bioheat equation considering body-core temperature elevation due to RF energy. In most conventional studies, the blood temperature is assumed to be constant over time. We considered that the blood temperature is spatially constant but as a variable over time. This assumption would be reasonable when discussing the human safety against the temperature elevation due to RF energy. Under the assumption, the term associated with blood perfusion was found to behave as a heat source for typical sets of thermal parameters, resulting in unphysical time evolution of blood temperature.

In order to overcome this difficulty, the computational procedure for compensating that artifact has been discussed. The effect for the discretization scheme associated with heat conduction has also been investigated, since it has been pointed out to cause computational error in the recent literature (Bernardi *et al* 2003, Samaras *et al* 2006).

We revealed that the dominant factor influencing the computed core temperature is the computational scheme for calculating the net rate of heat acquisition by blood from the body. The computed core temperature even for sets of thermal parameters which do not achieve balance was found to be reasonable once that scheme was introduced. An additional factor is the discretization scheme for the heat conductivity which has been proposed in recent literature (Bernardi *et al* 2003, Samaras *et al* 2006). This would also suppress the computational results.

Acknowledgement

This work was supported in part by the Strategic Information and Communications R&D Promotion Programme (SCOPE), Japan.

References

- Adair E R and Black D R 2003 Thermoregulatory responses to RF energy absorption *Bioelectromagnetics Suppl.* **6** S17-S38
- Bernarid P, Cavagnaro M, Pisa S and Piuze E 2003 Specific absorption rate and temperature elevation in a subject exposed in the far-field of radio-frequency sources operating in the 10-900-MHz range *IEEE Trans. Biomed. Eng.* **50** 295-304
- Ebert S, Eom S J, Schuderer J, Spostel U, Tillmann T, Dasenbrock C and Kuster N 2005 Response, thermal regulatory threshold of restrained RF-exposed mice at 905 MHz *Phys. Med. Biol.* **50** 203-5215
- Follow B and Neil E (ed) 1971 Circulation, Oxford University Press (New York USA)
- Gordon R G, Roemer R B, and Horvath S. M. 1976 A mathematical model of the human temperature regulatory system—transient cold exposure response *IEEE Trans. Biomed. Eng.*, **23**, 434–444
- Guy A W, Lin J C, Kramar P O and Emery A 1975 Effect of 2450-MHz radiation on the rabbit eye,” *IEEE Trans. Microwave Theory & Tech.* **23** 492-498
- Hirata A, Watanabe S, Kojima M, Hata I, Wake K, Taki M, Sasaki K, Fujiwara O and Shiozawa T 2006b Computational verification of anesthesia effect on temperature variations in rabbit eyes exposed to 2.45-GHz microwave energy *Bioelectromagnetics* **27** 602-612
- Hirata A, Asano T and Fujiwara O 2007 FDTD analysis of human body-core temperature elevation due to RF far-field energy prescribed in ICNIRP guidelines *Phys. Med. Biol.* **52** 5013-5023
- Hirata A, Sugiyama H, Kojoma M, Kawai H, Yamashiro Y, Fujiwara O, Watanabe S and Sasaki K 2008a Computational model for calculating body-core temperature elevation in rabbits due to whole-body exposure at 2.45 GHz *Phys. Med. Biol.* **53** 3391-3404
- Hirata A, Asano T, Fujiwara O 2008b FDTD analysis of body-core temperature elevation in children and adults for whole-body exposure *Phys. Med. Biol.* **53** 5223-5238
- ICNIRP 1998 Guidelines for limiting exposure to time-varying electric, magnetic and electromagnetic fields (up to 300 GHz),” *Health Phys.* **74** 494-522
- Kotte A, van Leeuwen G, deBree J, van der Koijk J, Crezee H and Lagendijk J 1996 A

description of discrete vessel segments in thermal modeling of tissues *Phys. Med. Biol.* **41** 865-84

Nelson D A 1998 Invited editorial on Pennes' 1948 paper revisited *J. Appl. Physiol.* **86** 2-3

Neufeld E, Chavannes N, Samaras T and Kuster N 2007 Novel conformal technique to reduce staircasing artifacts at material boundaries for FDTD modeling of the bioheat equation *Phys. Med. Biol.* **52** 4371-4381

Nguyen U D, Brown J S, Chang I A, Krycia J, Mirotznik M S 2004 Numerical evaluation of heating of human head due to magnetic resonance image. *IEEE Trans. Biomed Eng.* **51** 1301-1309

Pennes H H 1948 Analysis of tissue and arterial blood temperature in resting forearm *J. Appl. Physiol.* **1** 93-122

Saito K, Yoshimura H, Ito K, Aoyagi Y and Horita H 2004 Clinical trials of interstitial microwave hyperthermia by use of coaxial-slot antenna with two slots *IEEE Trans. Microwave Theory & Tech.* **52** 1987-1991

Samaras T, Christ A and Kuster N 2006 Effects of geometry discretization aspects on the numerical solution of the bioheat transfer equation with the FDTD technique *Phys. Med. Biol.* **51** 221-229

Wainwright P R 2003 The relationship of temperature rise to specific absorption rate and current in the human leg for exposure to electromagnetic radiation in the high frequency band *Phys. Med. Biol.* **48** 3143-3155

Wake K, Hongo H, Watanabe S, Taki M, Kamimura Y, Yamanaka Y, Uno T, Kojima M, Hata I and Sasaki K. 2007 Development of a 2.45-GHz local exposure system for in vivo study on ocular effects *IEEE Trans Microwave Theory & Tech.* **55** 588-596

Wissler E H 1998 Pennes' 1948 paper revisited *J. Appl. Physiol.* **85** 35-41

Fig. 1. Volume or surface integrated powers in equations (1) and (2) for different heat transfer coefficients. Solid and dotted lines represent the computational results with improved discretization scheme by Bernardi *et al* (2003) and Samaras *et al* (2006) and those with the conventional modeling. Powers in rabbit become balanced at the heat transfer coefficient $H=0.76 \text{ W m}^{-2} \text{ K}^{-1}$.

Fig. 2. Blood temperature elevation in the rabbit due to RF energy: (a) heat transfer coefficient $H=0.8 \text{ W m}^{-2} \text{ K}^{-1}$ with improved discretization scheme, (b) $H=1.5 \text{ W m}^{-2} \text{ K}^{-1}$ with improved discretization scheme, (c) $H=0.8 \text{ W m}^{-2} \text{ K}^{-1}$ with conventional discretization scheme, and (d) $H=1.5 \text{ W m}^{-2} \text{ K}^{-1}$ with conventional discretization scheme.

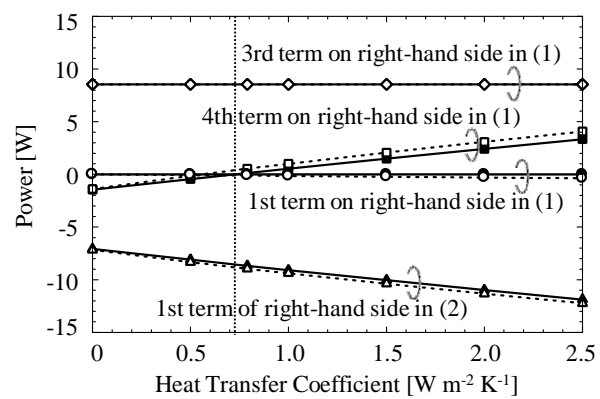


Fig. 1

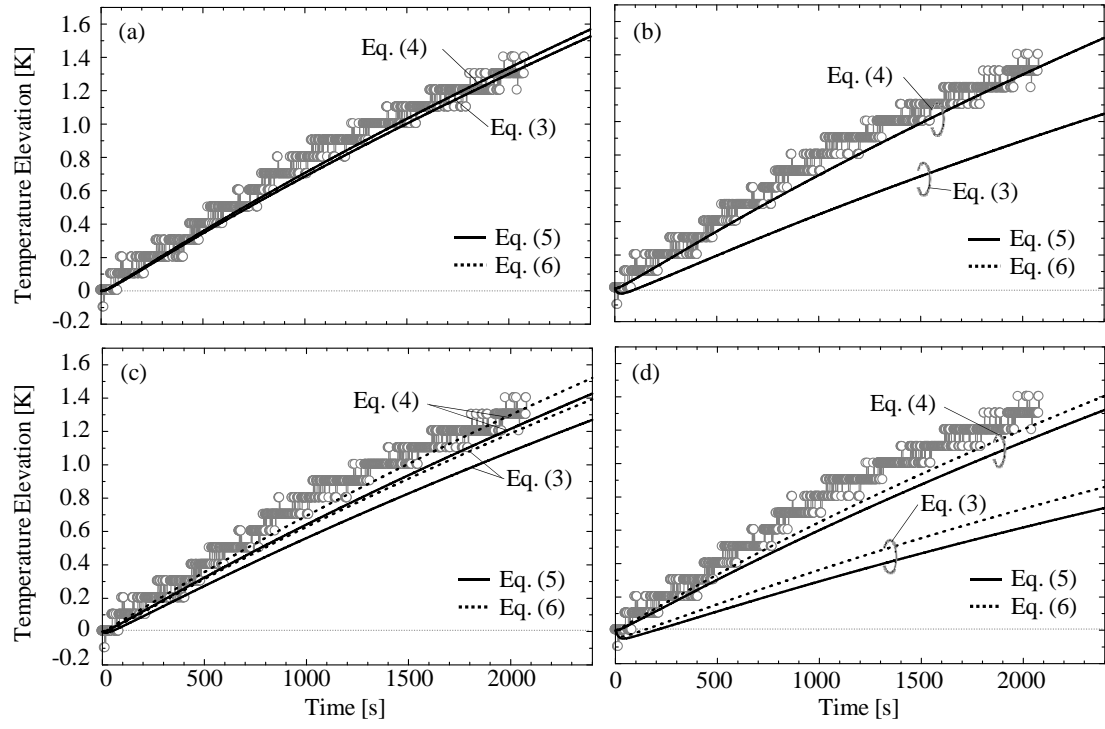


Fig. 2